Geol Rundsch (1994) 83: 514–522

M. Sultan · R. D. Tucker · Z. El Alfy · R. Attia
A. G. Ragab

U–Pb (zircon) ages for the gneissic terrane west of the Nile, southern Egypt

Received: 30 October 1993 / Accepted: 27 March 1994

Abstract The first U–Pb zircon ages are reported for the gneissic bedrock inliers previously interpreted as part of the Nile Craton. The inliers crop out in the Egyptian Western Desert, east of the Uweinat area and west of the Eastern Desert. Multi- and single-grain zircon analyses of granitoid gneiss and migmatite from Gebel Um Shagir, Aswan, and another locality approximately 160 km south-west of Aswan, yield simple discordia with near modern day Pb loss trajectories, and the following Neoproterozoic crystallization ages: $626 +4/-3$, 634 ± 4 and 741 ± 3 Ma. In contrast, multi- and single-grain U–Pb analyses (zircon and sphene) from an anorthositic gabbro at Gebel Kamil (22° 46′ N 26° 21′ E) and an anorthosite at Gebel El Asr (22° 46′ N 31° 10′ E) yield Archean and Paleoproterozoic emplacement ages. The former yield a crystallization age of > 2.67 Ga and a metamorphic age of ≈ 2.0 Ga; the latter a metamorphic age of 0.69 Ga and an inheritance age of 1.9–2.1 Ga. Because high grade gneiss and migmatite of Neoproterozoic, Paleoproterozoic and Archean age crop out west of the Nile, pre-Neoproterozoic crust should no longer be identified by its metamorphic grade. By contrast, mapping the anorthosite and related rocks might provide first-order estimates for the extension of pre-Neoproterozoic crust in north-east Africa. It is suggested that Archean and Paleoproterozoic crust of the Uweinat and Congo Craton are contiguous because these U–Pb (zircon) data show no evidence for a Neoproterozoic thermal overprint in the Gebel Kamil area and there is no pronounced Neoproterozoic magmatic activity south of the Uweinat inlier and north of the Congo Craton.

M. Sultan (✉) · R. D. Tucker
Washington University, Department of Earth and Planetary Sciences, St Louis, MO 63130, USA

Z. El Alfy
Egyptian Geological Survey and Mining Authority, 3 Salah Salem Street, Cairo, Egypt

R. Attia · Abdel Ghany Ragab
Ain Shams University, School of Science, Department of Geology, Abbassia, Cairo, Egypt

Key words Archean · Paleoproterozoic · Western Desert · Anorthosite · U–Pb (zircon) ages

Introduction

Neoproterozoic (550–900 Ma) volcanosedimentary rock units crop out along the Red Sea coast in Egypt, Sudan, Ethiopia and Saudi Arabia. The outcrops consist largely of low-grade greenschist facies, arc-related successions and interleaving belts of ophiolitic rocks, collectively known as the Arabian–Nubian Shield (ANS). Accretionary models for the ANS assume that an eastern (present day directions) complex of island arcs and intervening oceanic basins assembled and accreted against the Nile Craton in Neoproterozoic time. Areas identified as part of the Nile Craton are composed largely of migmatite, gneiss, charnockite and granulite primarily of quartzofeldspathic composition, with minor intercalations of quartzite, marble, calc-silicates and amphibolite (Klerkx, 1980; Schandelmeier et al., 1987; 1988).

Aside from differences in composition and metamorphic grade, the bedrock east and west of the River Nile are also different isotopically. Rocks west of the Nile have old depleted mantle model ages (T_{DM}) (Nelson and Depaolo, 1985), whereas to the east young model ages are present. For example, an orthogneiss from Bir Safsaf and two migmatites from Gebel El Asr have (T_{DM}) model ages of 1.55, 1.94 and 2.65 Ga, respectively, and seven granitic gneisses from southern Egypt and northern Sudan, west of the River Nile, yield (T_{DM}) model ages ranging from 1.6 to 2.6 Ga (Schandelmeier et al., 1988; Harms et al., 1990). These old model ages contrast with younger model ages (0.54–0.75 Ga) measured for samples from the Eastern Desert of Egypt and the Red Sea Hills of Sudan (Fig. 1) (Pegram et al., 1980; Sultan et al., 1990; Stern and Kröner, 1993). In addition, the initial Pb isotopic compositions of alkali feldspar from Neoproterozoic granitic rocks in the Eastern Desert define two geographical provinces: samples closest to Aswan (G. El Hudi, Aswan, Wadi Mariya; Fig. 1) are more radiogenic (initial

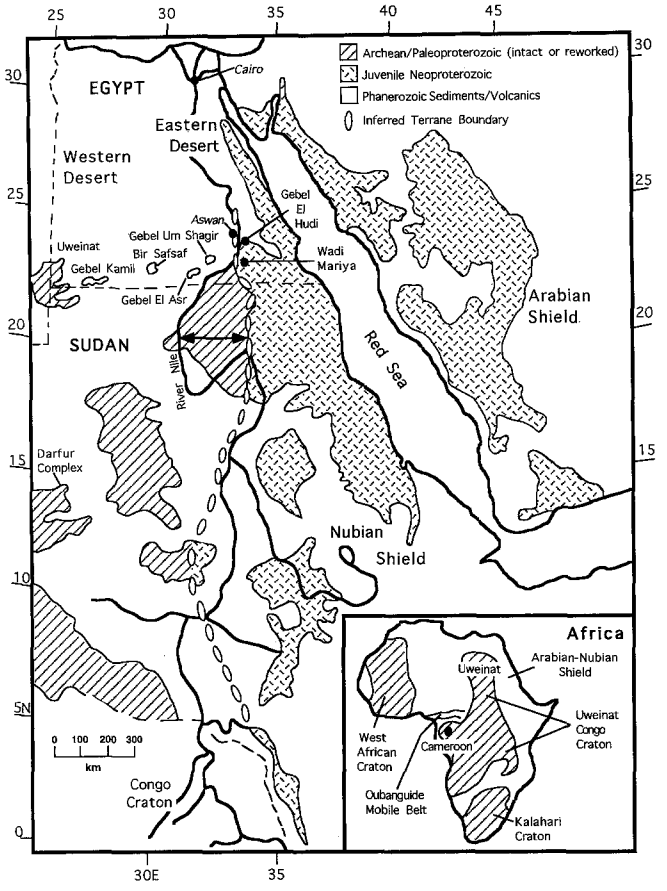

Fig. 1. Distribution of Archean–Paleoproterozoic and Neoproterozoic outcrops in north-east Africa. Also shown is the inferred boundary (Dixon and Golombek, 1988; Abdelsalam and Dawoud, 1991) between terranes formed largely of Archean– Paleoproterozoic crust (west) and areas formed mostly of Neoproterozoic juvenile crust. Deviations (indicated by double-headed arrow) from the boundary were exemplified by the discovery of a suture zone in northern Sudan that extends to areas previously identified as being part of the Nile Craton (Schandelmeier et al., 1993). Note that the boundary projects southward along the eastern margin of the Congo Craton. Lower right: inset showing distribution of cratons and selected mobile belts within Africa

$^{207}Pb/^{204}Pb = 15.611-15.629$) than samples from the east that display near-model mantle Pb isotopic compositions (Sultan et al., 1992). The large variations in Nd model ages and Pb isotopic compositions may indicate the presence of juvenile Neoproterozoic crust in the east and older crust in the west. Alternatively, the isotopic variations may indicate extensive assimilation by Neoproterozoic magmas of large amounts of older crust west of the River Nile. Reliable geochronological data are needed to differentiate between these interpretations.

Published isotopic ages, mostly utilizing whole rock Rb/Sr data, have established that the ANS formed between 900 and 550 Ma with little or no interaction with older crust. In contrast, the gneissic terrane west of the Nile is largely unexamined because of its inaccessibility and extensive Phanerozoic sedimentary cover. Pre-Neoproterozoic crust was documented in the Uweinat area (Fig. 1), about 600 km west of the exposed ANS. Whole rock Rb/Sr isochron ages for granulites (Karkur Murr series) from the Uweinat area and for anatectic granites and tonalites (Ayn Daw series) from the same area yielded 2656 ± 71 and 1836 ± 43 Ma ages, respectively (Klerkx, 1980; Cahen et al., 1984). Attempts to date other gneisses east of Uweinat using the Rb/Sr whole rock technique did not yield meaningful isochrons because of the extreme compositional heterogeneity of the gneisses (Stern et al., 1994), or possibly because the isotopic system was partially reset by Neoproterozoic metamorphic event(s) (Schandelmeier et al., 1987). Other Rb/Sr analyses yielded Neoproterozoic (562–918 Ma) errorchrons; the Neoproterozoic ages were interpreted as resetting ages (Harms et al., 1990).

Although no pre-Neoproterozoic crust has been reported east of the Uweinat, Archean and Paleoproterozoic crust is assumed to extend as far east as the River Nile (e.g., Dixon and Golombek, 1988). In this manuscript, we provide the first U–Pb (zircon) data from the gneissic terrane of the Western Desert of Egypt from Gebel Kamil, Gebel El Asr, Aswan, south-west Aswan and Gebel Um Shagir (Fig. 1). Our objective was to sample the major gneissic rocks west of the River Nile for U–Pb geochronology to understand the principle ages of the old cratonal rocks and to address the areal extent, assembly and evolution of the Nile Craton and adjoining terranes. Conventional U–Pb (zircon) geochronology holds the best promise for deciphering the distribution of crustal age provinces and for deciphering the tectonothermal history of the gneissic terrane of south-west Egypt.

Geological setting

Inliers of basement in the Western Desert include Gebel Kamil, Bir Safsaf, Gebel El Asr and Gebel Um Shagir (Fig. 1). We sampled a gabbroic anorthosite (78% plagioclase; 22% hornblende, chlorite and opaque phases) from Gebel Kamil (≈ 500 km west of the Nile) and an anorthosite (93% plagioclase; 7% hornblende) from Gebel El Asr (≈ 100 km west of the Nile), where field relations suggest that they are among the oldest units which can be dated. Our field observations in the Gebel Kamil and Gebel El Asr areas and published field and $P-T$ estimates (Bernau et al., 1987; Schandelmeier et al., 1987) reveal similarities with Archean high grade terranes elsewhere. The rock units are conformable, the metamorphic grade is upper amphibolite to granulite facies, quartzo feldspathic gneiss forms approximately 60–70% of the region and supracrustal rocks, including magnetite banded iron formations, and layered igneous complexes are common. The layered igneous complexes include pyroxenite, gabbro, leucogabbro and anorthosite. Within the complexes, gabbroid rock units are closely intermixed with, and grade into, anorthositic units. Anorthosites are common in Gebel El Asr, whereas in Gebel Kamil gabbroid rock units are dominant with only minor

Table 1. Whole rock major and trace element data, gneissic terrane

	RT-WD-4 Gebel Kamil	RT-Z-2 Gebel El Asr	RT-Z-1 Gebel Um Shagir	RT-Z-5 SW Aswan	RT-Z-7 Aswan
SiO_2	51.9	48.79	75.0	71.03	70.4
TiO_2	0.563	0.123	0.148	0.243	0.498
Al_2O_3	22.0	28.57	13.8	15.65	14.46
Fe_2O_3	6.48	2.7	1.081	2.65	3.14
MnO	0.07	0.044	0.025	0.077	0.033
MgO	2.73	2.05	0.26	0.911	0.79
CaO	9.92	14.24	1.17	4.09	1.97
Na_2O	4.52	2.77	3.74	4.08	3.33
K_2O	0.81	0.286	4.88	1.03	4.66
P_2O_5	0.08	0.0	0.049	0.11	0.13
LOI	0.95	0.26	0.29	0.28	0.63
Total	100.023	99.83	100.44	100.15	100.04
Ba	258 ± 15	134 ± 7	512 ± 11	284 ± 9	1774 ± 18
Rb	23 ± 2	3.9 ± 0.9	140 ± 1	14.4 ± 0.7	106 ± 1
Sr	605 ± 2	302 ± 1	100 ± 1	364 ± 2	1774 ± 17
Nb	2.4 ± 0.7	n.d.	11.5 ± 0.5	1.2 ± 0.6	13.4 ± 0.6
Zr	51 ± 1	13.4 ± 8	117 ± 1	61 ± 0.8	343 ± 1
V	100 ± 3	29 ± 2	3 ± 2	26 ± 2	24 ± 2
Co	31.9 ± 0.3	11.98 ± 0.12	7 ± 2	3.6 ± 1.8	5 ± 2
Ni	70 ± 18	48 ± 9	3 ± 1	0.0	6 ± 2
Ga	19.9 ± 0.9	15.3 ± 0.8	18 ± 1	14.7 ± 0.7	18.3 ± 0.8
Pb	16.3 ± 2.6	n.d.	22 ± 2	n.d.	11 ± 2

Ba, Rb, Sr, Nb, Zr, V, Co, Ni, Ga and Pb in ppm; rest in wt. %. Analyses were by X-ray fluorescence or INAA. Analytical uncertainties of the procedures are as follows (one standard deviation, percentage relative to reported values): < 1%, SiO_2, Al_2O_3, Fe_2O_3, CaO, K_2O; 1–5%, TiO_2, Na_2O; 5–15%, MnO, MgO; and 15–20%, P_2O_5.

intercalations of anorthosite. The layered complexes cover approximately 200 and 400 km^2 in Gebel El Asr and Gebel Kamil, respectively. Post-tectonic granodiorite and K-rich granite are ubiquitous within the Gebel El Asr area, but they are typically absent in the Gebel Kamil area. We collected an anorthosite from Gebel Kamil and a gabbroic anorthosite from Gebel El Asr. Both samples are fine- to medium-grained (typically 2 to < 1 mm), weakly banded and exhibit a well developed granoblastic texture.

The dominant rock types in Aswan, south-west Aswan and Gebel Um Shagir include migmatite, gneiss and migmatitic gneiss; post-tectonic granitic intrusive bodies, dikes, and sills are also common. We collected a granitic migmatite from Gebel Um Shagir area and a granite gneiss from an outcrop south-west of Aswan. Another granite gneiss was collected from within Aswan city. No post-tectonic plutons were sampled.

Samples from Aswan, south-west Aswan and Gebel Um Shagir are fine- to medium-grained biotite granite (quartz, orthoclase, plagioclase ± microline, perthite, hornblende, chlorite, sphene and opaque phases). Two (RT-Z-1, RT-Z-5) of the three samples contain garnet. A biotite granite gneiss (RT-Z-7) was collected from an old quarry within Aswan city in the vicinity of the unfinished obelisk. With the exception of a few felsic dikes, the biotite gneiss was the only rock type exposed in the quarry and in patchy outcrops nearby. Another biotite granite gneiss (RT-Z-5) was collected from an outcrop south-west of Aswan. The outcrop is 160 km from Aswan measured along the Aswan/Abu-Simbel asphalt road and 20 km east of the road. Low-lying hills (15–20 m high) trend east–west over an area 3 × 5 km wide. Granite gneiss is the dominant (≈ 60% of the outcrop) rock type; migmatites are less common. A granitic migmatite (RT-Z-1) was collected 7–8 km to the east of Gebel Um Shagir. Crystalline basement crops out over an area 30 × 15 km wide. Compositional banding within the migmatite ranges from millimetres to centimetres in thickness. Migmatite, gneiss and post-tectonic intrusions are dominant with minor intercalations of amphibolite, calc-silicate rock and marble (Bernau et al., 1987). Whole rock major and trace element compositions for the samples from Aswan, south-west Aswan and Um Shagir samples are given in Table 1.

Experimental techniques

Rocks were pulverized and sieved to a fine powder (< 70 μm) and separated into their mineral constituents by standard techniques. Selection of submilligram mineral fractions was carried out by hand-picking, with care taken to select only those grains devoid of inclusions and foreign minerals. Between 20 and 50 grains of clear, crack-free zircon comprised the average fraction, and all grains were strongly polished in an air-abrasion mill to reduce discordance and minimize ambiguity of the isotopic age.

Zircon was dissolved in a concentrated HF and HNO_3 acid solution after adding a trace amount of a mixed $^{205}Pb-^{235}U$ tracer solution. Extraction of U and Pb from zircon followed the method of Krogh (1973) but was performed in miniaturized exchange columns scaled down to one-tenth the published resin volume. Extraction of Pb and U from sphene was performed on a 3 ml ion-exchange column using a modified version of the procedure described by Corfu (1988). For common Pb values below 8 pg, we assigned the isotopic composition of the laboratory blank ($^{206}Pb/^{204}Pb = 18.3$; $^{208}Pb/^{206}Pb = 2.056$), whereas common Pb in excess of 8 pg was given an isotopic composition calculated from the Stacey and Kramers (1975) growth curve at the indicated age of the rock. Zircon analyses were corrected for 0.5 pg of U blank; sphene analyses were corrected for 5 pg of U blank.

Mass spectrometry was performed on a VG 354 thermal ionization mass spectrometer at the Geochronology Laboratory at the Royal Ontario Museum. Pb and U were loaded together onto Re filaments with silica gel and phosphoric acid and measurements were made by the peak-hopping method using the Daly collector. The Daly mass discrimination factor has been continously monitored and has remained constant at 0.38 ± .02/AMU over a period of several years and the correction for

Table 2. U–Pb and Sm–Nd data, gneissic terrane

Fractions			Concentrations			Th/U model[§]	Atomic ratios				Age (Ma)
Sample No.	Properties*	Wt. (μg)[+]	Pb rad (ppm)[+]	U (ppm)[+]	Pb common (pg)[‡]		$^{207}Pb/^{204}Pb''$	$^{207}Pb/^{206}Pb''$	$^{206}Pb/^{238}U''$	$^{207}Pb/^{235}U''$	$^{207}Pb/^{206}Pb''$
Gebel Kamil (RT-WD-4)**											
1	1 gr, pp, cl, fr	1	386	666	2	0.658	1604	0.17758 ± 23	0.4923 ± 19	12.0557 ± 518	2630
2	1 gr, pb, cl	2	382	691	4	0.481	1960	0.17727 ± 15	0.4878 ± 21	11.9251 ± 515	2628
3	1 gr, cl, c, r-p	9	2	5	2	0.074	66	0.12749 ± 47	0.3763 ± 72	6.6157 ± 411	2064
4	1 gr, cl, c, r-p	12	4	11	4	0.024	117	0.12668 ± 63	0.3729 ± 36	6.5133 ± 694	2052
5	+100, cl, f, p	51	4	12	5	0.060	360	0.12544 ± 17	0.3629 ± 15	6.2767 ± 284	2035
6	+200, cl, f, p	126	2	7	4	0.067	570	0.12396 ± 21	0.3465 ± 30	5.9216 ± 290	2014
7	−200, cl, c, r	105	9	27	9	0.108	755	0.12107 ± 16	0.3272 ± 11	5.4628 ± 208	1972
8	−100, cl, pb, sph	147	153	325	562	1.399	238	0.11939 ± 7	0.3520 ± 73	5.7941 ± 133	1947
9	−100, cl, pb, sph	158	213	462	653	1.370	307	0.11937 ± 28	0.3504 ± 26	5.7676 ± 439	1947
Gebel El Asr (RT-Z-2)**,++											
10	1 gr, +100 cl, c	8	12	46	2	0.275	342	0.11783 ± 15	0.2542 ± 9	4.1306 ± 178	1924
11	1 gr, +100, cl, c	5	15	73	3	0.482	168	0.09881 ± 16	0.2018 ± 8	2.7490 ± 117	1602
12	−200, cl, sub, eq	67	17	115	2	0.106	3062	0.08339 ± 12	0.1472 ± 5	1.6926 ± 62	1279
13	−200, cl, eq	66	14	104	13	0.081	345	0.07721 ± 6	0.1350 ± 5	1.4368 ± 58	1127
14	−200, cl, c, r	11	23	179	3	0.079	356	0.07161 ± 10	0.1284 ± 4	1.2674 ± 48	975
15	+200, cl, r	52	15	134	3	0.071	1074	0.06800 ± 10	0.1193 ± 4	1.1189 ± 42	869
16	db sph	69	51	418	82	1.232	145	0.06007 ± 12	0.0985 ± 2	0.8155 ± 40	606
17	db sph	293	19	186	99	1.450	215	0.05992±6	0.0970 ± 4	0.8015 ± 30	601
South-west Aswan (RT-Z-5)											
18	1 gr, +150, cl, c, sp	25	13	114	2	0.212	576	0.06404 ± 9	0.1212 ± 4	1.0699 ± 36	743
19	9 gr, +75, cl, c, sp	57	14	121	3	0.244	1075	0.06391 ± 8	0.1211 ± 4	1.0668 ± 39	739
20	+75, cl, c, t-rp	31	12	107	3	0.196	596	0.06389 ± 9	0.1199 ± 5	1.0559 ± 49	738
21	−75, c, r, sp	61	14	127	1	0.176	4551	0.06383 ± 9	0.1183 ± 4	1.0415 ± 42	736
22	−75, cl, c, t-p	45	14	127	2	0.159	995	0.06332 ± 10	0.1166 ± 4	1.0180 ± 34	719
Aswan City (RT-Z-7)											
23	+75, cl, c, n	88	53	502	92	0.474	200	0.06094 ± 11	0.1015 ± 4	0.8526 ± 34	637
24	1gr, +75, cl, c, sp	10	14	134	3	0.645	161	0.06093 ± 16	0.1003 ± 4	0.8429 ± 37	637
25	−75, cl, c, n	51	56	542	17	0.443	652	0.06085 ± 11	0.1013 ± 4	0.8503 ± 33	634
Gebel Um Shagir (RT-Z-1)											
26	−75, cl, cr, lp	15	207	2093	29	0.277	423	0.06058 ± 8	0.1000 ± 4	0.8355 ± 31	624
27	−75, cl, cr, lp	10	161	1661	21	0.324	309	0.06058 ± 10	0.0969 ± 3	0.8097 ± 29	624
28	−75, cl, cr, mp-p	27	196	2150	64	0.251	334	0.06049 ± 10	0.0925 ± 4	0.7717 ± 32	621
29	−75, cl, cr, lp	24	185	2033	78	0.234	234	0.06046 ± 10	0.0922 ± 3	0.7685 ± 30	620

* 1 gr denotes a single zircon grain analyzed. All other analyses are multi-grain zircon or sphene fractions selected from non-paramagnetic mineral separates at 0° tilt at full magnetic field in Frantz Magnetic Separator; 100, 200 = size in mesh (200 mesh = 75 μm); c = colorless; cl = clear; cr = cracked; db = dark brown; el = elongate; eq = equant; f = faceted; fr = zircon fragment; lp = long prismatic; mp-p = middle parts of prisms; n = 5:1 prismatic needles; p = prismatic; pb = pale brown; pp = pale pink; r = rounded; r-p = rounded prismatic; sp = short prismatic; sph = sphene; sub = subhedral; t-p = tips broken from prisms; t-rp = tips broken from round prismatic; t-crp = tips broken from cracked prisms; pb = pale brown. Standard analytical techniques are given in Krogh (1973). All grains air-abraded following Krogh (1982).

[+] Concentrations are known to ±30% for sample weights ≧ 20 μg and ± 50% for samples ≦ 5 μg.

[‡] Corrected for 0.0215 mole fraction common Pb in the ^{205}Pb-^{235}U spike.

[§] Calculated Th/U ratio assuming that all ^{206}Pb in excess of blank, common Pb and spike is radiogenic ($\lambda^{232}Th = 4.9475 \times 10^{-11} y^{-1}$).

[′] Measured, uncorrected ratio.

[″] Ratio corrected for fractionation, spike, blank, and initial common Pb at the determined age from Stacey and Kramers (1975). Pb and U fractionation correction = 0.1%/amu (± 0.14%); U blank = 0.5 pg, Pb blank ≦ 10 pg. Absolute uncertainties (2σ) in the Pb/U and $^{207}Pb/^{206}Pb$ ratios were calculated following Ludwig (1980) using known U and Pb half-lives and isotopic abundance ratios from Jaffey et al. (1971).

** Modal abundance of mafics in Gebel Kamil and Gebel El Asr samples, respectively: 20–24 and 5–10. An content (Plagioclase) = 46–54, 70–81 respectively.

++ Sm–Nd data for Gebel El Asr. Sm = 0.3513 ± 7; Nd = 1.2690 ± 13; $^{147}Sm/^{144}Nd = 0.1674$; $^{143}Nd/^{144}Nd = 0.512194 \pm 15$; ε_{Nd}(Today) = −8.7 ± 3; ε_{Nd}(690 Ma) = −6.1. Sm/Nd ratios corrected for instrumental discrimination based in $^{146}Nd/^{144}Nd = 0.7219$. Concentrations in ppm and uncertainties at 2σ. Sm–Nd data were generated at Washington University. Analytical procedures from Pier et al. (1989).

thermal mass fractionation is 0.13%/AMU. Errors quoted in Table 2 include measurement uncertainties and uncertainty in the instrumental mass fractionation calculated after the method of Ludwig (1980). Decay constants and isotopic abundance ratios are those of Jaffey et al (1971) as recommended by the IUGS Subcommission on Geolochronology (Steiger and Jäger, 1977).

Fresh samples weighing 2 to 5 kg were collected, crushed and pulverized to less than 170 mesh using a Spex Shatterbox with an alumina mortar. All reported whole rock major and trace element compositions were determined using an automated Siemens SRS-2000 X-ray spectrometer at Washington University. The accuracy and precision of the method were monitored by including masked standards with each run of samples.

Plagioclase analyses were performed using a fully automated JEOL 733 Superprobe with three wavelength-dispersive spectrometers. An accelerating voltage of 15 kV and a current of 20–50 nA were the standard operating conditions. Natural mineral standards were used for calibration and to monitor the accuracy and precision during data acquisition.

Geochronological data

Analytical results for the Gebel Kamil and El Asr samples are presented in Table 2 and portrayed in Figs 2 and 3, respectively; results for the Aswan, south-west Aswan and Gebel Um Shagir samples are given in Table 2 and illustrated in Fig. 4. All error ellipses are shown at the two sigma confidence level and linear regressions were carried out using the program of Davis (1982). Age errors are given at the 95% confidence level.

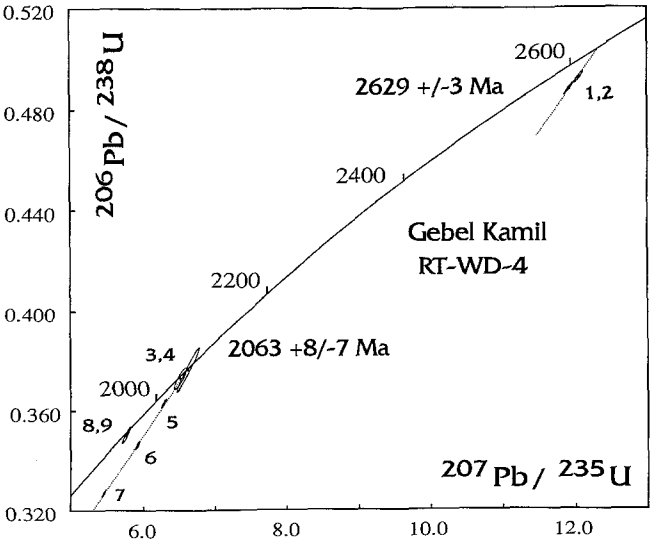

Fig. 2. Concordia diagram of U–Pb isotopic data for a gabbroic anorthosite from Gebel Kamil. Data points are numbered as in Table 2

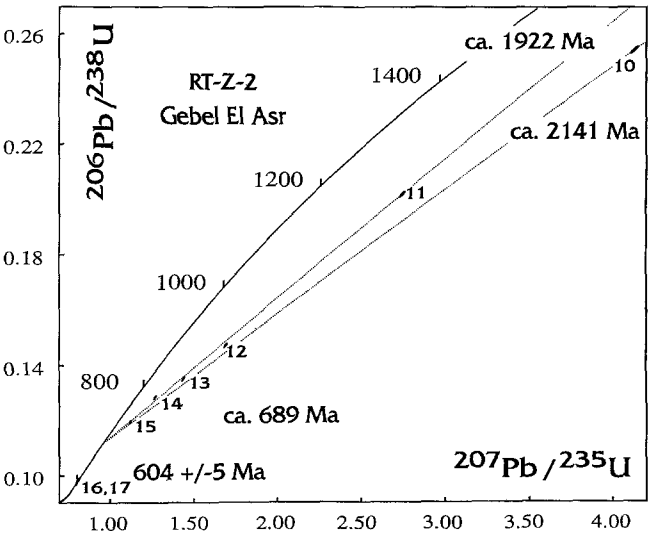

Fig. 3. Concordia diagram of U–Pb isotopic data for an anorthosite from Gebel El Asr. Data points are numbered as in Table 2

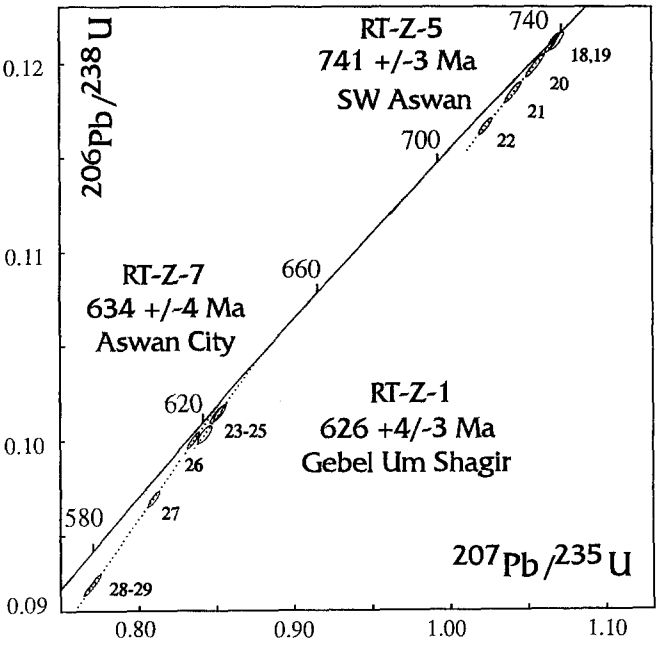

Fig. 4. Concordia diagram of U–Pb isotopic data for a migmatite from Gebel Um Shagir, a granite gneiss from south-west Aswan and another from Aswan. Data points are numbered as in Table 2

Gebel Kamil (RT-WD-4)

Most zircons in the Gebel Kamil anorthosite are clear, equant and multifaceted crystals, approximately 150–75 μm in diameter. A few (< 10%) are pale pink to pale brown in color, subrounded and subhedral in habit and approximately 200 μm in diameter. Two single-grain analyses (Nos. 1, 2; Table 2, Fig. 2) of colored zircon yield identical $^{207}Pb/^{206}Pb$ ages of 2629 ± 3 Ma; three multigrain fractions (Nos. 5–7; Table 2, Fig. 2) and two single grains (Nos. 3, 4; Table 2, Fig. 2) of the clear zircon type

define a discordia with an upper intercept age of 2063 +8/−7 Ma and a poorly defined Neoproterozoic lower intercept age. The five analyses (Nos. 3−7; Table 2, Fig. 2) are 0.3, 1.9, 6.5, 14.1 and 22.9% discordant, respectively, and fall on a line with a 37% probability that scatter is due to measurement error alone. Two multigrain fractions (Nos. 8, 9; Table 2, Fig. 2) of euhedral sphene yield a concordant age of ca. 1947 Ma.

Two interpretations for the zircon data for Gebel Kamil are possible: (1) the rock is an Archean gabbroic anorthosite, metamorphosed in the Paleoproterozoic (2063 Ma for the time of zircon growth and 1947 for the time of sphene formation), or (2) the rock is a Paleoproterozoic (2063 Ma) gabbroic anorthosite, with inherited, xenocrystic Archean zircon (2629 Ma), metamorphosed at 1947 Ma. In interpretation 1 above, the minimum and maximum ages of emplacement are 2629 Ma and 2741 Ma, respectively. The minimum age of emplacement is obtained from the $^{207}Pb/^{206}Pb$ ages of analyses 1 and 2, which are 2630 and 2628 Ma, respectively. The maximum age was defined by the upper intercept of a discordia extrapolated from the time of metamorphism (2063 Ma) through analyses 1 and 2. In interpretation 2, the age of emplacement (2063 Ma) is the upper intercept of a discordia defined by analyses 3−7. The minimum age of inherited zircon is ca. 2629 Ma, the $^{207}Pb/^{206}Pb$ age of analyses 1 and 2. We prefer interpretation 1 for two reasons: (1) anorthosite rarely contains xenocrystic zircon and (2) the morphology, low U abundance (5−27 ppm) and low model Th/U ratio (Th/U = 0.02−0.1) of the clear zircons are consistent with a metamorphic origin (Percival and Krogh, 1983; Corfu, 1988; Kamo and Davis, 1994). Because Th is not readily soluble in aqueous fluids, zircons that crystallize from a metamorphic fluid will usually show fairly low Th/U values.

Gebel El Asr (RT-Z-2)

Four multi-grain (Nos. 12−15; Table 2, Fig. 3) and two single zircon analyses (Nos. 10, 11; Table 2, Fig. 3) from Gebel El Asr anorthosite define a wedge-shaped array with a Neoproterozoic (ca. 689 Ma) lower intercept age and a range of Paleoproterozoic (1922−2141 Ma) upper intercept ages (Fig. 3). The $^{207}Pb/^{206}Pb$ ages for the zircon analyses range between 1924 and 869 Ma, and two multi-grain sphene analyses (Nos. 16, 17; Table 2, Fig. 3) define a mean age of 604 ± 5 Ma. As with Gebel Kamil, the dominant zircons in the Gebel El Asr sample are equant, multifaceted, and low in Th relative to U, suggestive of a metamorphic origin. Five (Nos. 11−15; Table 2, Fig. 3) of the six zircon analyses define a discordia that intersects concordia at 689 and 1922 Ma with 62, 86, 91, 95 and 97% discordance, respectively. A line through the 689 Ma lower intercept and the sixth zircon analysis (No. 10; Table 2, Fig. 3) intersects the concordia at 2141 Ma. Moreover, the most discordant zircon analyses with the oldest $^{207}Pb/^{206}Pb$ ages have the highest Th/U ratios (Th/U = 0.3−0.5) compared with the zircon fractions with younger $^{207}Pb/^{206}Pb$ ages (Th/U = 0.08−0.1), suggesting that the most discordant analyses have the largest component of inherited igneous-type zircon cores (Fig. 3).

The Gebel El Asr zircon array is therefore interpreted as a mixture of: (1) inherited zircon with minimum ages ranging from 2.1 to 1.9 Ga and Th/U ratios consistent with an igneous origin and (2) younger metamorphic zircon (with depleted Th/U ratio) dated at 689 Ma. Because there is considerable scatter in the data (Fig. 3), a more complex interpretation is possible. For example, such scatter could occur if the Gebel El Asr anorthosite witnessed two or more metamorphic events: (1) the 1.9−2.0 Ga metamorphic event(s) detected at Gebel Kamil, and (2) Neoproterozoic event(s) detected from the zircon data (689 Ma) and sphene data at Gebel El Asr. The multi-grain sphene analyses yield an age of 604 ± 5 Ma best interpreted as the age of the last metamorphic event in Gebel El Asr area. The complex metamorphic history that we advocate implies an older emplacement age, a suggestion that is supported by the calcic nature of the plagioclase (An content = 70−81) typical of Archean anorthosites and is consistent with the Sm−Nd data. The initial whole rock $\varepsilon_{Nd} = -6.1$ at 690 Ma and Sm−Nd depleted mantle model age [TDM] (Nelson and De Paolo, 1985) is 2845 Ma (caption of Table 2).

South-west Aswan granite (RT-Z-5)

This granite yielded a moderate amount of zircon grains which range from equant and subrounded to long and subrounded. They are typically colorless, and most grains in the least magnetic mineral fraction are crack-free with no obvious sign of inherited cores or younger overgrowths.

Five small fractions of zircon were analyzed; each fraction consisted of less than 40 grains and the weight of each fraction was between 62 and 25 μg. One analysis is concordant at ca. 743 Ma, and if regressed with the four other slightly discordant analyses an emplacement age of 741 ± 3 Ma is indicated (Fig. 4).

Aswan City (RT-Z-7)

This granite gneiss yielded a rich population of small (< 150 μm) long-prismatic and needle-like zircon (length/width > 4); fewer short-prismatic grains are also present. All morphological types are generally clear and colorless and they are best interpreted as comprising a single igneous population. Two small fractions of needle-like zircon, together with a fraction of short-prismatic grains, form a collinear array with 1.5−2.5% discordance indicating an emplacement age of 634 ± 4 Ma (Fig. 4).

Gebel Um Shagir (RT-Z-1)

This granite gneiss yielded a moderate amount of zircon, dominantly of the long-prismatic variety, with rounded tips and aspect ratios in excess of five. Four analyses of

colorless needle-like zircon indicate an emplacement age of 626 +4/−3 Ma (Fig. 4). All analyses are slightly discordant, having experienced 2−9% Pb loss, probably because of their moderately high U abundances and resultant radiation damage.

Discussion

Anorthosites occur within Archean high grade terranes, Proterozoic (massif-type) anorthosite, less often, in layered mafic intrusions, within ophiolitic sequences, or as inclusions within igneous rocks (Ashwal, 1993). Two lines of evidence suggest that the anorthosite from Gebel El Asr and the gabbroic anorthosite from Gebel Kamil may be of Archean age. Firstly, the Gebel Kamil gabbroic anorthosite is shown to have an Archean zircon component with a minimum crystallization age of 2.67 Ga. Although the oldest zircons from Gebel El Asr fall on hypothetical mixing lines to minimum ages of 2.1 and 1.9 Ga, an Archean emplacement age cannot be ruled out (see above). Secondly, plagioclase from Gebel El Asr is fairly calcic (An content 70−81), as is the case with many Archean anorthosites elsewhere. Plagioclase from Gebel Kamil has been extensively ($\approx$ 40%) altered to epidote that lowers the An component of the plagioclase on its formation. This explains why plagioclase from Gebel Kamil does not display typical Archean An contents but rather has a value of An 46−54.

The age groupings reported in the previous section correspond to compositional variations. Neoproterozoic samples are K-rich granites, whereas the Archean to Paleoproterozoic samples are anorthositic in composition. These results and our field observations indicate that pre-Neoproterozoic anorthosite and related rocks occur west of the Nile. Because many anorthosites world-wide are Archean to Mesoproterozoic in age (Ashwal, 1993), mapping their distribution in north-east Africa might give first-order estimates for the extension of the pre-Neoproterozoic crust in this area.

Differences in composition, metamorphic grade and isotopic affinities between the ANS and the gneissic terrane were used to outline the approximate location of the boundary between the Nubian Shield and the Nile Craton. As described earlier, the River Nile separates to a first approximation high grade gneisses and migmatites in the west from low grade volcanosedimentary arc terranes to the east. Our results indicate that the terrane west of the River Nile consists of high grade gneisses and migmatites that are either Neoproterozoic, Paleoproterozoic or Archean in age. Before our work all of the high grade gneisses and migmatites would have been generally considered as being of pre-Neoproterozoic age. The presence of high grade gneisses should be no longer used as a criterion for defining areas that are of pre-Neoproterozoic age.

A north−south trending boundary that broadly follows the River Nile (longitude 34°) was found to separate areas with low initial $^{87}Sr/^{86}Sr$ and $^{207}Pb/^{204}Pb$ and positive ε_{Nd} values to the east from areas with high initial $^{87}Sr/^{86}Sr$ and $^{207}Pb/^{204}Pb$ and negative ε_{Nd} values to the west. The former areas were assumed to be underlain by Archean and Paleoproterozoic crust, the latter by juvenile Neoproterozoic crust (Dixon and Golombek, 1988). Whereas the Pb, Nd and Sr data provided first-order understanding of variations in the isotopic compositions of crustal provinces in north-east Africa, inferences from these data regarding the precise location of the boundary should be considered with caution. We cite four reasons for our concerns. Firstly, large variations in the ε_{Nd} values and initial Pb isotopic compositions could indicate older crust in the west and younger crust in the east, but they may also be explained by variations in the amounts of recycled older crust. Secondly, many areas, especially to the south, are poorly sampled. Thirdly, the boundary between the ANS and the older crust was defined using arbitrary cutoff values for the initial Sr, Nd and Pb isotopic compositions. Varying these values would shift the boundary from its present location. Fourthly, there could be detached fragments of the Nile Craton, now embedded in Neoproterozoic crust. For example, Gebel El Asr could be a detached fragment from the Uweinat inlier. Failure to identify these fragments complicates the identification of the boundary location. Given these uncertainties, we suspect that the boundary is likely to be irregular, occasionally deviating from the straight line advocated by Dixon and Golombek (1988). We note, for example, the recent discovery of a suture zone in northern Sudan that extends to areas previously identified on the basis of geological and isotopic data as being part of the Nile Craton (Schandelmeier et al., 1993). The boundary is here redefined as a zone that is formed largely of remobilized, remelted, reworked or intact Archean to Late Proterozoic crustal components, which separates areas largely made of juvenile Neoproterozoic rocks (east) from intact older crust (west).

In a deviation from tectonic models that treat the terrane west of the Nile as a craton, Black and Liegois (1993) suggest that this area experienced 'decratonization' during the Neoproterozoic. They propose that the Nile Craton lost its thick mechanical boundary layer and was thus subject to hot asthenospheric upwellings which left behind an extensive old reactivated terrane extending from Libya across western Sudan and Egypt, Chad and Central African Republic to the Congo. Within these areas they cite the following features in support of their hypothesis: widespread Phanerozoic anorogenic alkaline magmatism, abundant late tectonic high K calc-alkaline magmatism, reactivated Archean and Paleoproterozoic crust, ophiolitic nappes and major Pan-African shear zones along the boundaries of the Nile Craton and/or surrounding cratons.

This is an intriguing model, but the present isotopic data and field observations west of the Nile do not allow such inferences to be drawn. We do not know, for example, the extent to which the Uweinat inlier extends southward. U−Pb (zircon) results suggest that the Neoproterozoic thermal overprint did not affect the Gebel

Kamil area (Sultan et al., 1994). To the best of our knowledge, there is no pronounced Neoproterozoic magmatic activity south of the Uweinat and north of the Congo Craton (Vail, 1989). The similarity in isotopic ages between the Gebel Kamil and Gebel El Asr samples and those reported from southern Cameroon (Van Schmus and Toteu, 1992) supports earlier suggestions (e.g. Kröner, 1977; Vail, 1991) that the Congo and Nile Cratons are contiguous. Van Schmus and Toteu (1992) identified the Ebolowa charnockite as the oldest unit (≈ 2.9 Ga) and they detected a thermal overprint and plutonic activity at 2.0–2.1 Ga by dating metamorphic zircon in the nearby Nyong gneiss series. They reported 2.5–3.0 Ga Nd mantle separation ages for the charnockite and the gneiss, and they detected a Neoproterozoic thermal overprint at ca. 600 Ma. Thus the continuity of pre-Neoproterozoic crust between the Unweinat inlier and the Congo Craton could not be ruled out given the available data. We suggest the term Uweinat-Congo Craton for this area (Fig. 1, inset). Our model could be further tested by examining the lithological and geochronological affinities of the Darfur complex south of Uweinat and north of the Congo craton (Fig. 1). Our model predicts that the complex is part of the Uweinat-Congo Craton.

Conclusions

1. We report the first conventional U–Pb (zircon and sphene) data for five samples collected from the gneissic terrane west of the Nile. One of the investigated samples is a gabbroic anorthosite from Gebel Kamil and another is an anorthosite from Gebel El Asr. The remaining samples are biotite granite gneiss (Aswan and south-west Aswan) and migmatite (Gebel Um Shagir). The Gebel Kamil and Gebel El Asr anorthosites yield Archean and Paleoproterozoic crystallization ages, respectively; the remaining samples yield Neoproterozoic emplacement ages.
2. The Gebel Kamil data are best interpreted as indicating a minimum emplacement age of 2629 Ma of a gabbroic anorthosite that was metamorphosed in the Paleoproterozoic (2063 Ma for the time of zircon growth and 1947 for the time of sphene formation). The Gebel El Asr zircon array is interpreted as a mixture of (a) inherited zircon with minimum ages ranging from 2.1 to 1.9 Ga and with Th/U ratios consistent with an igneous origin and (b) younger metamorphic zircon (with depleted Th/U ratio) dated at 689 Ma.
3. A biotite granite gneiss from Aswan, a granitic migmatite from Gebel Um Shagir and a biotite granite gneiss from south-west Aswan yield the following emplacement ages: Aswan: 634 ± 4 Ma; Gebel Um Shagir: $626 +4/-3$ Ma; south-west Aswan: 741 ± 3 Ma.
4. Our results show that the terrane west of the Nile comprises high grade gneiss and migmatite of Neoproterozoic, Paleoproterozoic and Archean age. The presence of high grade gneiss should be no longer used as a criterion for defining areas that are of pre-Neoproterozoic age.
5. Results suggest that Archean and Paleoproterozoic anorthosite and related rocks occur west of the Nile. Because many anorthosites world-wide are Archean to Mesoproterozoic in age, mapping their distribution in north-east Africa might give first-order estimates for the extension of the pre-Neoproterozoic crust in the area.
6. We suggest that the pre-Neoproterozoic crust extends between the Uweinat and the Congo Craton via the Darfur complex because our U–Pb (zircon) data show no evidence for a Neoproterozoic thermal overprint in the Gebel Kamil area. Also no pronounced Neoproterozoic magmatic activity was reported south of the Uweinat and north of the Congo Craton. Because we do not know how far east and west the Uweinat extends, we prefer to name this section of Archean and Paleoproterozoic crust the Uweinat–Congo Craton.

Acknowledgements Supported by NASA Geology Program grant contract NAGW 1358 to Washington University and NSF grant contract INT-9313017 to Washington University. We thank M. Bassiouni, A Dardir, G. Naim and I. Shalaby for logistical support for field work in Egypt, R. E. Arvidson, R. J. Stern and H. Schandelmeier for constructive comments, R. Couture for conducting whole rock major and trace element analyses, D. Kremser for conducting microprobe analyses and T. E. Krogh for facilitating the use of the Royal Ontario Museum laboratories for dating the Egyptian samples.

References

Abdelsalam MG, Dawoud AS (1991) The Kabus ophiolitic melange, Sudan, and its bearing on the western boundary of the Nubian Shield. J Geol Soc London 148: 83–92

Ashwal LD (1993) Anorthosites. Springer-Verlag Berlin Heidelberg, pp 1–422

Bernau R, Darbyshire DPF, Franz G, Harms U, Huth A, Mansour N, Pasteels P, Schandelmeier H (1987) Petrology, geochemistry and structural development of the Bir Safsaf-Aswan uplift, southern Egypt. J Afr Earth Sci 6: 79–90

Black R, Liegeois J-P (1993) Cratons, mobile belts, alkaline rocks and continental lithospheric mantle: the Pan-African testimony. J Geol Soc London 150: 89–98

Cahen L, Snelling NJ, Delhal J, Vail JR (1984) The Geochronology and Evolution of Africa. Clarendon Press, Oxford, pp 1–512

Corfu F (1988) Differential response of U–Pb systems in coexisting accessory minerals, Winnipeg River subprovince, Canadian Shield: implications for Archean crustal growth and stabilization. Contrib Mineral Petrol 98: 312–325

Davis DW (1982) Optimum linear regression and error estimation applied to U–Pb data. Can J Earth Sci 19: 2141–2149

Dixon TH, Golombek MP (1988) Late Precambrian crustal accretion rates in northeast Africa and Arabia. Geology 16: 991–994

Harms U, Schandelmeier H, Darbyshire DPF (1990) Pan-African reworked early/middle Proterozoic crust in NE Africa west of the Nile: Sr and Nd isotope evidence. J Geol Soc London 147: 859–872

Jaffey AH, Flynn KF, Glendenin LE, Bently WC, Essling AM (1971) Precision measurements of the half-lives and specific activities of ^{235}U and ^{238}U. Phys Rev C4: 1889–1906

Kamo SL, Davis DW (1994) Reassessment of Archean crustal development in the Barberton Mountain Land, South Africa, based on U–Pb dating. Tectonics 13: 167–192

Klerkx J (1980) Age and metamorphic evolution of the basement complex around Jabal al 'Awaynat. In: Salem MJ, Busrewil M (eds) The Geology of Libya 3. Academic Press New York, pp 901–906

Krogh TE (1973) A low contamination method for hydrothermal decomposition of zircon and extraction of U and Pb for isotopic age determinations. Geochim Cosmochim Acta 37: 488–494

Krogh TE (1982) Improved accuracy of U–Pb zircon dating by selection of more concordant fractions using a high gradient magnetic separation technique. Geochim Cosmochim Acta 46: 637–649

Kröner A (1977) The Precambrian geotectonic evolution of Africa: plate accretion vs. plate destruction. Precambrian Res 4: 163–213

Ludwig KR (1980) Calculation of uncertainties of U–Pb isotope data. Earth Planet Sci Lett 46: 212–220

Nelson BK, Depaolo DJ (1985) Rapid production of continental crust 1.7 to 1.9 b.y. ago: Nd isotopic evidence from the basement of the North American mid-continent. Geol Soc Am Bull 96: 746–754

Pegram WJ, Sando TW, Hodges KV (1980) Rare-earth element geochemistry and Nd isotopic composition of some Egyptian Younger granites. Geol Soc Am Abst Prog 12: 497

Percival JA, Krogh TE (1983) U–Pb zircon geochronology of the Kapuskasing structural zone and vicinity in the Chapleau–Foleyet area, Ontario. Can J Earth Sci 20: 830–843

Pier JG, Podosek FA, Luhr JF, Brannon JC, Arnada-Gomez JJ (1989) Spinel-lherzolite-bearing Quaternary volcanic centers in San Luis Potosi, Mexico: II. Sr and Nd isotopic systematics. J Geophys Res 94: 7941–7951

Schandelmeier H, Richter A, Harms U (1987) Outline of the geology of magmatic and metamorphic units between Gebel Uweinat and Bir Safsaf (SW Egypt/NW Sudan). Tectonophysics 140: 233–246

Schandelmeier H, Darbyshire DPF, Harms U, Richter A (1988) The East Saharan Craton: evidence for pre-Pan-African crust in NE Africa west of the Nile. In: El-Gaby S, Greiling RO (eds) The Pan African Belt of Northeast Africa and Adjacent Areas. Friedr Vieweg, Braunschweig, pp 69–94

Schandelmeier H, Kuster D, Wipfler E, Abdel Rahman EM, Stern RJ, Abdelsalam MG, Sultan M (1993) Evidence for a new late Proterozoic suture in northern Sudan. In: Thorweihe U Schandelmeier H (eds) Geoscientific Research in Northeast Africa. Balkema, Rotterdam, pp 83–85.

Stacey JS, Kramers JD (1975) Approximation of terrestrial lead isotope evolution by a two-stage model. Earth Planet Sci Lett 26: 207–221

Steiger RH, Jäger E (1977) Subcomission on geochronology: convention on the use of decay constants in geo- and cosmochronology. Earth Planet Sci Lett 36: 359–362

Stern RJ, Hedge CE (1985) Geochronologic and isotopic constraints on late Precambrian crustal evolution in the Eastern Desert of Egypt. Am J Sci 285: 97–127

Stern RJ, Kröner A (1993) Late Precambrian crustal evolution in NE Sudan: isotopic and geochronologic constraints. J Geol 101: 555–574

Stern RJ, Kröner A, Reischman T, Bender R, Dawoud AS (1994) Precambrian basement around Wadi Halfa, Sudan: a new perspective on the evolution of the East Saharan Craton. Geol Rundsch 83: 564–577

Sultan M, Chamberlain KR, Bowring SA, Arvidson RE, Abuzied H, El Kaliouby B (1990) Geochronologic and isotopic evidence for involvement of pre-Pan-African crust in the Nubian Shield, Egypt. Geology 18: 761–764

Sultan M, Bickford ME, El Kaliouby B, Arvidson RE (1992) Common Pb systematics of Precambrian granitic rocks of the Nubian Shield (Egypt) and tectonic implications. Geol Soc Am Bull 104: 456–470

Vail JR (1989) Ring complexes and related rocks in Africa. J Afr Earth Sci 8: 19–40

Vail JR (1991) The Precambrian tectonic structure of North Africa. In: Salem MD, Sbeta AM (eds) The Geology of Libya 6, Elsevier, Amsterdam New York, pp 2259–2268

Van Schmus WR, Toteu SF (1992) Were the Congo Craton and the Sao Francisco Craton joined during the fusion of Gondwanaland? Eos 73: 365